Performance of IEEE 802.15.4a UWB WBAN Receivers in a Real Hospital Environment

Ville Niemelä[1], Alberto Rabbachin[2], *Member*, IEEE, Attaphongse Taparugssanagorn[1], *Member*, IEEE, Matti Hämäläinen[1], *Senior Member*, IEEE, Jari Iinatti[1], *Senior Member*, IEEE

[1]Centre for Wireless Communications
University of Oulu
Oulu, Finland

[2]Institute for the Protection and the Security of Citizen
Joint Research Centre
Ispra, Italy

***Abstract*—In the near future, especially in the developed countries, the number of elder people is increasing. There is a need for improving the methods used in the welfare and healthcare to be able to threat the patients with the same or even less amount of nursing staff than nowadays. Adapting wireless technology into the medical sector is one potential way to improve the methods. Having a vest of wireless sensors on the patient's body would enable not only online measurements of physiological parameters such as heart rate, body temperature or even electrocardiograph (ECG) but also free mobility of the patients, yet another factor to improve the recovery process. In this paper, ultra wideband (UWB) simulations according to the IEEE 802.15.4a are presented with wireless body area network (WBAN) channel models measured in a real hospital environment in Oulu, Finland.**

I. INTRODUCTION

A picture of the future is that a wireless medical environment is utilized in different surroundings. Whether it is a hospital room, a bedroom at home or an ambulance, the basic idea is the same. There is a wireless sensor network measuring physiological parameters of a human body, transmitting the measured data to an access point in a close proximity of the body and from the access point the data is forwarded through different media like wireless local area network (WLAN) to a database which is accessed by the nursing staff, doctors and nurses. The most important aspects are that executing the measurements with wireless equipment is simpler and easier, it can be done online and the measurements allow patients to perform everyday tasks like going to a bathroom or getting a cold drink from a fridge, not to mention that all the information would be available for a nursing staff in real time. For medical staff this means savings in working time from writing down measurement results or doing the different measurements by hands to actual nursing [1]. For patients it means shorter and easier recovery periods since it is possible to do wireless measurements enabling free mobility which is desired in the most cases of healing processes. In addition to both of these, a new technology can help cutting down the increasing costs of the healthcare sector.

As a technology for WBAN, UWB provides many advantages over the other techniques, like Bluetooth. UWB has a low emission power level which means a long battery life and low power spectral density which is a safety issue when working on a close proximity of a human body. UWB transmission can be on a baseband frequency. This means not only simpler and lower-cost receivers since there is no need for up- or down conversion of the signal but also savings in the power consumption. [2]

UWB propagation channel studies have been performed in the recent years [3-5] and it has been proved that the channel characteristics are different when the transmission is effected by a human body. With its complex shape and different tissues each with different permittivity has an impact on the propagation. Also the environment effects the UWB propagation in WBAN [6-7]. UWB simulations carried out earlier are not based on any standard and the used WBAN channel models are not specified in a real medical environment. [8]

In this paper we are concentrating on UWB simulations according to the IEEE 802.15.4a standard for low-rate wireless personal area networks [9]. The aim was to build a UWB simulator according to a known standard to be able to compare different channel models and environments. WBAN is a part of the wireless personal area network and therefore IEEE 802.15.4a is suitable for the UWB WBAN simulations. Another reason is that the IEEE 802.15.6 [11] for WBAN has not been published yet, though the channel model for it was published in spring 2009 [12]. The measurement results [6] in a real hospital environment are being used here as a WBAN channel model when analyzing the results in different hospital environments between different types of receivers which can be implemented according to the IEEE 802.15.4a. Additional white Gaussian noise (AWGN) results are used for verification as reference results.

II. SYSTEM MODEL

The simulator has been implemented in Matlab© in time domain. It follows strictly the IEEE 802.15.4a standard requirements being an impulse radio signaling based UWB transceiver [9]. The transmitted UWB waveform during the k^{th} symbol interval can be expressed as [9]

$$x^{(\mathrm{k})}(t) = \left[1 - 2g_1^{(\mathrm{k})}\right] \sum_{n=1}^{N_{\mathrm{cpb}}} \left[1 - 2s_{\mathrm{n+kN_{cpb}}}\right] \times p\left(t - g_0^{(\mathrm{k})} T_{\mathrm{BPM}} - h^{(\mathrm{k})} T_{\mathrm{burst}} - nT_{\mathrm{c}}\right) \quad (1)$$

where $g_0^{(k)}$ is a position modulated bit and $g_1^{(k)}$ is a phase modulated bit. Sequence $s_{n+kN_{cpb}} \in \{0,1\}$, n = 0, 1, …, N_{cpb} –1 is the scrambling code used in the k^{th} interval and $h^{(k)}$ is the k^{th} burst hopping position also defined by the scrambler. $p(t)$ is the transmitted pulse waveform at the antenna input, T_{BPM} is the half length of a symbol defining the position of the burst in the symbol, T_{burst} is the length of a burst and T_c is the length of a pulse. The structure of a symbol is presented in Fig. 1. [9]

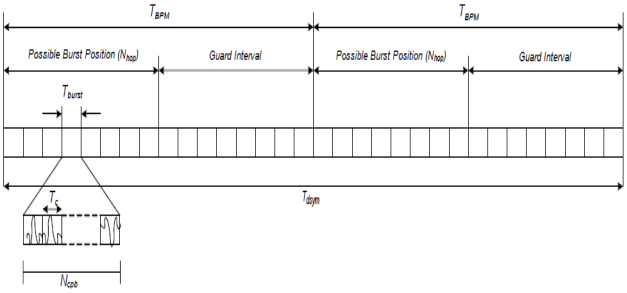

Figure 1. Structure of one UWB symbol in IEEE 802.15.4a.

According to the standard, the position modulated bits are always information bits and phase modulated bits redundant convolutional parity bits. With this modulation structure the information bits can be received by both coherent and non-coherent receivers. However, the coherent receiver can take the advantage from the convolutional encoding to improve its performance. Both receivers use Reed-Solomon coding. The Reed-Solomon encoded parity check bits are always position modulated, therefore visible for both types of the receivers. [9]

The k^{th} received symbol can be written as [10]

$$r^{(k)}(t) = x^{(k)}(t) * h(t) + n(t) \qquad (2)$$

where $x^{(k)}(t)$ is a transmitted signal as in (1), $h(t)$ is the channel impulse response, "*" states convolution and $n(t)$ is a white Gaussian noise.

In this paper, three different types of receivers are studied.

- A coherent receiver, presenting here a reference receiver with the best possible performance.
- A binary orthogonal non-coherent receiver with and without convolutional channel coding.
- An energy detector (ED).

Coherent detection is expressed as

$$v_i^{(k)} = \int_s^{s+nT_c} r(t-\tau)w(t)\,d\tau,\ i=0,1 \qquad (3)$$

where $w(t) = \sum_{n=1}^{N_{ncp}} \left(\left[1 - 2s_{n+kN_{cpb}}\right]\right) \times p(t - nT_c) * h(t)$, $s = k2T_{BPM} + iT_{BPM} + h^{(k)}T_{burst}$ and T_c is the length of one pulse. Executing $w(t)$ like this performs an all-rake receiver collecting all the possible multipath components of the transmitted signal.

In non-coherent receiver, the comparison of the absolute values defines which position modulated binary number has been received

$$\left|v_0^{(k)}\right| \underset{"1"}{\overset{"0"}{\gtrless}} \left|v_1^{(k)}\right| \qquad (4)$$

i.e., if $v_0^{(k)}$ is bigger than $v_1^{(k)}$, the received bit is "0". Otherwise it is "1". Note that, since the transmitted signal is also phase modulated, the detection of the position modulated bit has to be done in non-coherent manner.

The Viterbi decoder gets as an input the sequence of bits obtained by both position and phase modulated bits. The phase modulated bits are obtained by taking the correlation output described in (3) according to the burst position detected by using (4). The phase detection can be written as

$$v_0^{(k)}, v_1^{(k)} \underset{"0"}{\overset{"1"}{\gtrless}} 0 \qquad (5)$$

If the correlation output is bigger than zero the phase detected bit is "1", otherwise it's "0".

In ED, the received signal is first passed through a band-pass filter (BPF) in order to reduce the noise bandwidth. Assuming that the BPF won't cause distortion to the received signal, the decision variable for the position modulation can be written as

$$w_i^{(k)} = \int_s^{s+nT_c} r(t)^2\,dt,\ i=0,1 \qquad (6)$$

The decision on the received bit is based on the comparison between the decision variable and is expressed as

$$w_0^{(k)} \underset{"1"}{\overset{"0"}{\gtrless}} w_1^{(k)} \qquad (7)$$

For the ED, the integration time is defined by the length of the transmitted burst length. Due to channel effects and un-optimized integration times at the receiver, part of the energy of the signal is lost. Therefore in WBAN channel, the performance of the energy detector is expected to be somewhat worse than it could be.

A. WBAN channel model

WBAN channel model used in the simulations is based on the UWB measurement campaign in a real hospital environment in Oulu, Finland [6]. Inside the hospital, different surroundings were measured and were also simulated here.

Environment can be a regular hospital room, a hospital corridor or a surgery room. Position means that the measured patient is either lying down on a bed (or on a surgery table) or standing. For a link, there are two options: link A1 is a link between a sensor node in the middle of the torso and a sensor node on the left wrist. Link A2 is a link between a sensor

node on the left side of a torso and on top of a two meters height pole located two meters away from the person. [6]

B. Simulations

Signal-to-noise ratio (E_b/N_0) is used to present the results where E_b states energy of one bit, i.e., energy measured over one burst. E_b, whether only one pulse (2 ns) or 512 pulses, is always normalized to one. N_0 is a zero mean Gaussian noise. In all the simulations, 10^6 bits per one E_b/N_0 value were simulated. All different hospital scenarios, different symbol rates and number of users (N_{hop}) were covered. Different symbol rates and N_{hop} values can be seen in Table 1 [9].

Table 1. Simulations parameters.

Number of users	Symbol rate (MHz)	Pulses (2ns) per burst
N_{hop} = 2	0.12 0.98 7.80 31.20	N_{cpb}=512 N_{cpb}=64 N_{cpb}=8 N_{cpb}=2
N_{hop} = 8	0.12 0.98 7.80 15.60	N_{cpb}=128 N_{cpb}=16 N_{cpb}=2 N_{cpb}=1
N_{hop} = 32	0.12 0.98 1.95 3.90	N_{cpb}=32 N_{cpb}=4 N_{cpb}=2 N_{cpb}=1

Verification of the simulations was done by comparing the reference bit error rate (BER) curve without channel coding with the theoretical antipodal bit error probability curve. The curves were identical. In binary orthogonal non-coherent detection without channel coding, the difference to the theoretical antipodal bit error probability curve is 4 dB. In the simulations, using decision variables from (4) gave the same result.

III. RESULT COMPARISON

A. AWGN

Fig. 2 presents the simulation results in an AWGN channel. Red curves are coherent reference results which without a channel coding were used to verification. In the red curves the position modulated bit is assumed to be known and only the phase modulated bit is detected as in (3) and (5). In Fig. 2 N_{hop} = 8 and all four possible symbol rates were simulated (Table 1).

The blue curves in Fig. 2 are bit error rates of the ED. The differences in the blue curves are due to the receiver structure. The received signal samples are first squared and then integrated, as presented in (6). Therefore also the noise samples are first squared thus having more influence on the results as the burst length increases. With N_{hop} = 8 and symbol rate 0.12 MHz ED has 7-8 dB worse performance than the purple curves of the non-coherent detection which is not influenced of the increased burst length. For symbol rate 15.60 MHz, being a pulse position modulated signal (Table 1), the difference to non-coherently detected is less than 1 dB.

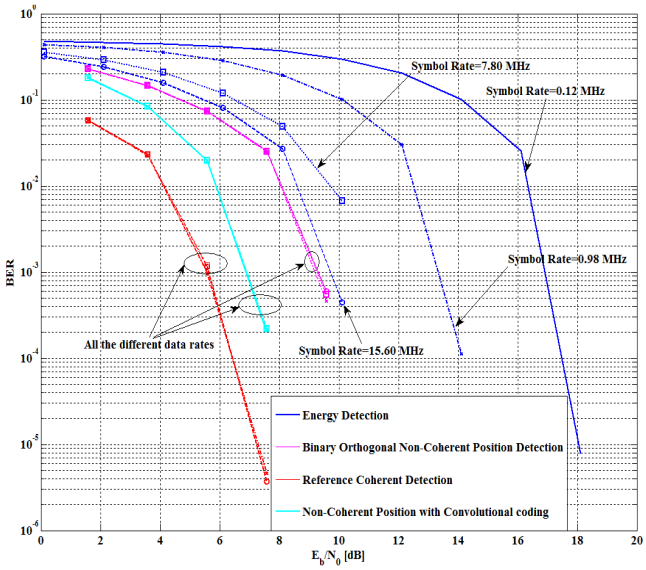

Figure 2. Different symbol rates in AWGN channel.

In light blue and purple curves, the position modulation is non-coherently detected. In the purple curve, only the position of the burst is being detected according to (3) and (4). Light blue curve includes convolutional coding which is added in the phase of a burst and detected coherently.

Coherent and the binary orthogonal non-coherent detections in AWGN channel on the other hand are not influenced by the differences in the burst lengths. The results are the same and independent of the burst duration.

Adding the convolutional coding and decoding it with Viterbi algorithm can improve the binary orthogonal non-coherent detection approximately 2 dB.

B. WBAN

Fig. 3 shows the difference in performance in AWGN and WBAN channel models when N_{hop} and symbol rate parameters are 8 and 0.98 MHz, respectively. Fig. 4 shows the results with different symbol rates when N_{hop} = 8. In WBAN channel model, the environment is a regular hospital room, the measured patient was lying down on a hospital bed and link is A1, from the middle of a torso to the left wrist.

The difference in performance between AWGN and WBAN is 4-5 dB in both coherent and non-coherent detection. In energy detection the difference is more, 7-8 dB. As explained before, both coherent and non-coherent detection benefit of the all-rake receiver. ED on the other hand "suffers" because the channel effects are ignored at the receiver, i.e., integration times of the bursts are not optimized and part of the energy of the burst is lost.

In Fig. 4, with WBAN channel model, there are variations among different symbol rates in the coherently and non-coherently detected curves, in contrary to AWGN channel model. Now longer bursts perform about 2.5 or 5 dB better than the two shorter bursts (symbol rate 7.8 MHz and 15.60 MHz).

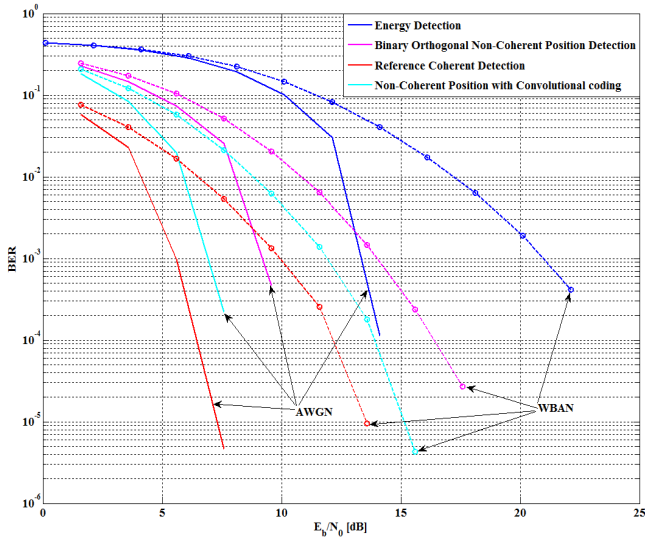

Figure 3. Performance in AWGN and WBAN channel models.

For ED, the influence is inversed. The performance of different length of bursts is getting closer to each other, the slowest symbol rate still being the worst with the most noise influencing. The advantage of the longer bursts in WBAN channel is due to the integration time. Since the integration time is not optimized at the receiver, the proportion of the lost energy of shorter bursts is bigger than with the longer bursts

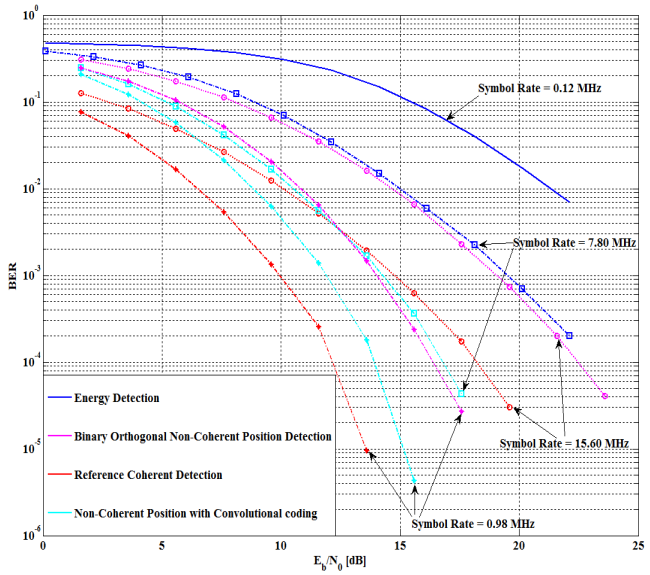

Figure 4. Performance of different symbol rates in WBAN channel.

IV. CONCLUSIONS

The results show performance of the systems built according to the IEEE 802.15.4a standard. Two different channel models were used, AWGN as for verification and a reference, and WBAN channel model to see how a low-complexity and low power receivers would perform in a real hospital environment.

Comparison of an ED, a non-coherent detector and a coherent detector was performed. Results show approximately 2 dB gain in a non-coherent case when convolutional coding is used. ED seems to perform, depending on the symbol rate, 2-7 dB worse than the non-coherent detector.

These results apply when there is a same transmission, and the detection of the signal is done coherently or non-coherently still retaining the same information. The difference between non-coherent detection with and without convolutional coding is around 2 dB. Without the convolutional coding both the transmitter and the receiver would be simpler and thus cheaper still remaining almost the same performance.

REFERENCES

[1] Rissanen H., Isokanniainen K., Pirinen P., Alasaarela E. (2006) Wilho – A New Concept of Wireless Management of Healthcare Processes. 6th Nordic Conference on eHealth and Telemedicine (NCeHT), Helsinki, Finland.

[2] Rabbachin A. (2008) Low complexity UWB receivers with ranging capabilities. Acta universitatis Ouluensis, Series C, Technica 298. University of Oulu, Oulu.

[3] Fort A., Desset C., Ryckaert J., De Doncker P., Van Biesen L., Wambacq P. (2006) Characterization of the Ultra Wideband Body Area Propagation Channel. IEEE International Conference on Ultra-Wideband, Zurich, Switzerland, 2005.

[4] Zasowski T., Meyer G., Althaus F., Wittneben A (2005). Propagation Effects in UWB Body Area Networks. IEEE International Conference on Ultra-Wideband. Zurich, Switzerland, 2005.

[5] Molisch A.F., Cassioli D., Chong C-C., Emami S., Fort A., Kannan B. et al. (2006) A Comprehensive Standardized Model for Ultrawideband Propagation Channels. IEEE Transactions on Antennas and Propagation, vol. 54.

[6] Taparugssanagorn A., Pomalaza-Raez C., Tesi R., Isola A., Hämäläinen M., Iinatti J.. (2009) UWB Channel for Wireless Body Area Networks in a Hospital Environment. The 12th International Symposium on Wireless Personal Multimedia Communications (WPMC'09), Sendai, Japan, Sep. 7-10, 2009.

[7] Ghassemzadeh S.S., Greenstein L.J., Kavcic A., Sveinsson T., Tarokh V. (2003) UWB Indoor Path Loss Model for Residential and Commercial Buildings. IEEE Vehicular Technology Conference 2003.

[8] Viittala H., Hämäläinen M., Iinatti J. (2008) Suitability Study of DS-UWB and UWB-FM for Medical Applications. The 11th International Symposium on Wireless Personal Multimedia Communications (WPMC), Saariselkä, Finland, Sep 8-11, 2008.

[9] IEEE Standard 802.15.4a: Part 15.4: Wireless Medium Access Control (MAC) and Physical Layer (PHY) Specifications for Low-Rate Wireless Personal Area Networks (WPANs), Amendment 1: Add Alternate PHYs. IEEE Computer Society, IEEE Std 802.15.4a–2007 (Amendment to IEEE Std 802.15.4 –2006), NY, USA. 187 p.

[10] Proakis J.G. & Salehi M. (2008) Digital Communications, Fifth Edition, McGraw-Hill, Inc., International Edition, New York.

[11] IEEE 802.15 WPAN Task Group 6 (TG6) Body Area Networks. http://www.ieee802.org/15/pub/TG6.html Page available at 1.2.2010.

[12] IEEE P802.15 Working Group for Wireless Personal Area Networks (WPANs). Channel Model for Body Area Network (BAN). (2009). IEEE 802.15.6 channel modeling subcommittee.